# Cluster Synchronization in Networks of Kuramoto Oscillators ⋆

**Chiara Favaretto** * **Angelo Cenedese** * **Fabio Pasqualetti** **

* *Department of Information Engineering, University of Padova, Italy (e-mail: chiara.favaretto.2@phd.unipd.it,angelo.cenedese@unipd.it)*
** *Department of Mechanical Engineering, University of California at Riverside, CA 92521 USA (e-mail: fabiopas@engr.ucr.edu)*

**Abstract:** A broad class of natural and man-made systems exhibits rich patterns of cluster synchronization in healthy and diseased states, where different groups of interconnected oscillators converge to cohesive yet distinct behaviors. To provide a rigorous characterization of cluster synchronization, we study networks of heterogeneous Kuramoto oscillators and we quantify how the intrinsic features of the oscillators and their interconnection parameters affect the formation and the stability of clustered configurations. Our analysis shows that cluster synchronization depends on a graded combination of strong intra-cluster and weak inter-cluster connections, similarity of the natural frequencies of the oscillators within each cluster, and heterogeneity of the natural frequencies of coupled oscillators belonging to different groups. The analysis leverages linear and nonlinear control theoretic tools, and it is numerically validated.

*Keywords:* Kuramoto Oscillators, Cluster Synchronization, Linear and Nonlinear Systems

## 1. INTRODUCTION

Synchronization of coupled oscillators is ubiquitous in nature (Lewis et al. (2014); Strogatz (2000)), from the cohesive flocking of birds (Giardina (2008)) to the orchestrated firing of neurons (Nordenfelt et al. (2013); Ferrari et al. (2015)) to the dynamics of man-made networks, including power grids and computer networks (Nishikawa and Motter (2015)). While some systems require synchronization of all units to function properly (Dörfler and Bullo (2014); Chopra and Spong (2005); Cenedese and Favaretto (2015); Gushchin et al. (2015)), recent studies have shown how neural systems, among others, depend on cluster synchronization, where populations of neurons evolve cohesively but independently from one another, and how incorrect patterns may prevent cognitive functions and characterize to degenerative states such as Parkinson's and Huntington's diseases (Hammond et al. (2007); Rubchinsky et al. (2012); Banaie et al. (2009)), and epilepsy (Lehnertz et al. (2009)). Despite recent results, e.g., Pecora et al. (2014); Sorrentino et al. (2016); Schaub et al. (2016), methods to predict and control cluster synchronization in dynamically-changing networks remain critically lacking.

In this paper we focus on networks of Kuramoto oscillators (Kuramoto (1975)), and we identify topological and intrinsic conditions leading to cluster synchronization. Our choice of Kuramoto dynamics is motivated by the broad applicability of this model to describe complex synchronization phenomena across different application domains (Ferrari et al. (2015); Dörfler and Bullo (2014); Gushchin et al. (2015); Kurz et al. (2015)). In this paper we show how cluster synchronization emerges when the coupling among a group of oscillators is sufficiently stronger than the coupling with the remaining oscillators, and the natural frequencies of the oscillators in the group are sufficiently homogeneous and different from the natural frequencies of the remaining oscillators. In fact, the larger the difference between the natural frequencies inside and outside the cluster, the more cohesive the evolution of cluster phases.

**Related work** Full synchronization in networks of Kuramoto oscillators has received considerable attention, e.g., see Dörfler and Bullo (2014). Typically, full synchronization is possible when the coupling among the oscillators is sufficiently strong to overcome the differences of the oscillators' natural frequencies. Partial or cluster synchronization has, instead, been the subject of few recent works. For instance, stability properties of patterns and group synchronization for different classes of dynamical systems is studied in Dahms et al. (2012). The relationship between clustered dynamics and the topology is analyzed in Lu et al. (2010), where the authors focus on nonidentical dynamical behaviors of different clusters. More recently, Burger et al. (2013) analyzes the clusterization in the asymptotic behavior, while Pecora et al. (2014) highlights how symmetry of the interconnection network may lead to cluster synchronization, and Sorrentino et al. (2016) exploits network symmetries to characterize all possible patterns of cluster synchronization in networks of oscillators coupled by a network with Laplacian matrix. Finally, more general network topologies are analysed in Schaub et al. (2016), where clusters are defined through the graph-theoretical notion of external equitable partitions. In this work, we depart from the above works by proposing and studying a relaxed notion of cluster synchronization, which applies to general networks and interconnection dynamics.

⋆ This material is based upon work supported in part by NSF awards BCS-1631112 and BCS-1430279.

**Paper contributions** The contribution of this paper is twofold. First, we propose a notion of cluster synchronization in networks of Kuramoto oscillators. With respect to existing notions of cluster synchronization where the phases of the clustered oscillators are required to be equal to each other, we define cluster synchronization when the phase differences remain bounded over time. This definition is less stringent, and it allows us to study cluster synchronization in asymmetric oscillatory networks with general topology and parameters. Second, we show how cluster synchronization depends on a graded combination of strong intra-cluster and weak inter-cluster connections, similarity of the natural frequencies of the oscillators within each cluster, and heterogeneity of the natural frequencies of coupled oscillators belonging to different groups. We provide two different results for the cohesiveness of the phases of the oscillators in a cluster. The first result is based on the nonlinear dynamics of the network, and it bounds from above the phase differences of the clustered oscillators. The second result uses a linear system to bound the nonlinear dynamics, and it approximates the phase differences of the clustered oscillators as a function of the network parameters and natural frequencies of the oscillators. Although our second result is an approximate bound, it provides novel insight into the mechanisms enabling cluster synchronization in oscillatory networks, and it serves as a tight indication of the nonlinear network evolution, as we show through a set of numerical studies.

**Paper organization** The remainder of the paper is organized as follows. Section 2 contains the problem setup and our main results on cluster synchronization in networks of Kuramoto oscillators. Section 3 contains our numerical studies, and finally Section 4 concludes the paper.

## 2. CLUSTER SYNCHRONIZATION IN NETWORKS OF KURAMOTO OSCILLATORS

### *2.1 Problem setting*

We consider a network of $n$ Kuramoto oscillators, represented by a weighted, undirected, and connected graph $\mathcal{G} = (\mathcal{V}, \mathcal{E})$, where $\mathcal{V} = \{1, \dots, n\}$ and $\mathcal{E} \subseteq \mathcal{V} \times \mathcal{V}$ denote the set of oscillators (nodes) and edges, respectively (Godsil and Royle (2001)). The matrix $A = [a_{ij}]$ denotes the adjacency matrix of $\mathcal{G}$, whose elements satisfy $a_{ij} \in \mathbb{R}_{\geq 0}$ if $(i,j) \in \mathcal{E}$ and $a_{ij} = 0$ otherwise. Let $\mathbb{S}^1$ denote the unit-radius circle. Each oscillator $i \in \mathcal{V}$ is described by a phase angle $\theta_i \in \mathbb{S}^1$, whose dynamics evolve as a heterogeneous Kuramoto system (Kuramoto (1975)):

$$\dot{\theta}_i = \omega_i + \sum_{j=1}^{n} a_{ij} \sin\left(\theta_j - \theta_i\right), \qquad i = 1, \dots, n, \tag{1}$$

where $\omega_i \in \mathbb{R}_{\geq 0}$ is the $i$-th natural frequency.

Let $|\theta_j - \theta_i|$ denote the geodesic distance between the two angles $\theta_i, \theta_j \in \mathbb{S}^1$. In this context (and with reference to Fig. 1), we introduce the following definition:

*Definition 1.* ***(Cluster of oscillators)*** The set of oscillators $\mathcal{C} \subseteq \mathcal{V}$ is a cluster if there exists an angle $0 \leq \gamma \leq \pi/2$ such that, if $|\theta_j(0) - \theta_i(0)| \leq \gamma$, then $|\theta_j(t) - \theta_i(t)| \leq \gamma$, for all $i, j \in \mathcal{C}$ and at all times $t \geq 0$. □

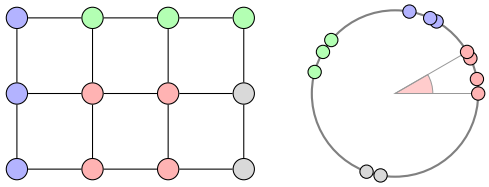

Fig. 1. The left figure shows a network of 12 oscillators with 4 color-coded clusters. The phases of the oscillators within each cluster evolve cohesively, as defined in Definition 1 and illustrated in the right figure.

Although Definition 1 allows a node to belong to different clusters, we will not discuss this case throughtout this paper, which is aimed at the characterization of a single cluster with respect to all the other nodes. Moreover, notice that frequencies need not be equal for nodes to belong to the same cluster.

Differently from the case of complete synchronization, the mechanisms enabling cluster synchronization in Kuramoto networks have not been thoroughly characterized. With this work, we characterize topological and intrinsic properties of the network leading to the emergence of clusters of oscillators, where the phase angles evolve coherently (in the sense of Definition 1) within a cluster, but independently among clusters. In particular, we show that clustered oscillators' dynamics are due to the interplay of the following network features: strong intra-cluster and weak inter-cluster connections, and natural frequencies that are relatively homogenous within each cluster and sufficiently different among oscillators in neighboring clusters.

### *2.2 Analysis based on nonlinear cluster dynamics*

Let $\mathcal{C} \subseteq \mathcal{V}$ denote a group of oscillators. From (1), the dynamics of each oscillator in $\mathcal{C}$ can be decomposed as

$$\dot{\theta}_i = \omega_i + \sum_{j \in \mathcal{C}} a_{ij} \sin\left(\theta_j - \theta_i\right) + \sum_{j \in \mathcal{V} \setminus \mathcal{C}} a_{ij} \sin\left(\theta_j - \theta_i\right). \tag{2}$$

Depending on the network parameters and oscillators' frequencies, the group $\mathcal{C}$ may behave as a cluster. In the next Theorem we further characterize this relation.

*Theorem 1.* ***(Cluster condition based on network weights and oscillators' frequencies)*** Let $\mathcal{C} \subseteq \mathcal{V}$ and

$$\alpha_{\max} = \max_{i,j \in \mathcal{C}} \left( \frac{\omega_{ij} + \sum_{k \in \mathcal{V} \setminus \mathcal{C}} \left(a_{jk} + a_{ik}\right)}{2a_{ij} + \sum_{k \in \mathcal{C}} \min\{a_{ik}, a_{jk}\}} \right),$$

where $\omega_{ij} = \omega_j - \omega_i$ and $a_{ij}$ are as in (1). If $\alpha_{\max} \leq 1$, then $\mathcal{C}$ is a cluster with respect to the angle

$$\gamma = \arcsin(\alpha_{\max}). \tag{3}$$

That is, if $|\theta_j(0) - \theta_i(0)| \leq \gamma$ for all $i, j \in \mathcal{C}$, then $|\theta_j(t) - \theta_i(t)| \leq \gamma$ for all $i, j \in \mathcal{C}$ and all times $t \geq 0$.

**Proof.** Let $\theta_{ij} = \theta_j - \theta_i$, and assume that $|\theta_{ij}(0)| \leq \gamma$ for all $i, j \in \mathcal{C}$. Notice that

$$\dot{\theta}_{ij} = \dot{\theta}_j - \dot{\theta}_i = \omega_{ij} + \sum_{k \in \mathcal{V}} a_{jk} \sin(\theta_{jk}) - a_{ik} \sin(\theta_{ik}).$$

We show that, whenever $|\theta_{ij}| = \gamma$ for some $i, j \in \mathcal{C}$, then $\frac{d|\theta_{ij}|}{dt} \leq 0$, thus proving the forward invariance of the angle $\gamma$. Assume that $\theta_{ij} = \gamma$ (the case $\theta_{ij} = -\gamma$ follows from analogous reasoning). We have

$$\dot{\theta}_{ij} = \omega_{ij} - 2a_{ij}\sin(\gamma) + \sum_{k\in\mathcal{V}\setminus\mathcal{C}} a_{jk}\sin(\theta_{jk}) - a_{ik}\sin(\theta_{ik}) + \sum_{k\in\mathcal{C}\setminus\{i,j\}} \underbrace{a_{jk}\sin(\theta_{jk}) - a_{ik}\sin(\theta_{ik})}_{f_k}.$$

Notice that for all $j,k = 1,\dots,n$, it is

$$\theta_{jk} = \theta_k - \theta_j = \theta_i - \theta_j + \theta_k - \theta_i = \theta_{ji} + \theta_{ik} = -\gamma + \theta_{ik},$$

where $\theta_{ij} = \gamma$ by assumption, and

$$\begin{aligned}\frac{\partial f_k}{\partial \theta_{ik}} &= a_{jk}\cos(\theta_{ik} - \gamma) - a_{ik}\cos(\theta_{ik}) \\ &= a_{jk}\cos(\theta_{ik})\cos(\gamma) + \sin(\theta_{ik})\sin(\gamma) - a_{ik}\cos(\theta_{ik}) \\ &= (a_{jk}\cos(\gamma) - a_{ik})\cos(\theta_{ik}) + \sin(\gamma)\sin(\theta_{ik}).\end{aligned}$$

Moreover,

$$\begin{cases} \dfrac{\partial f_k}{\partial \theta_{ik}} < 0, & \text{if } 0 \le \theta_{ik} < \arctan\left(\dfrac{a_{ik} - a_{jk}\cos(\gamma)}{\sin(\gamma)}\right), \\ \dfrac{\partial f_k}{\partial \theta_{ik}} > 0, & \text{if } \arctan\left(\dfrac{a_{ik} - a_{jk}\cos(\gamma)}{\sin(\gamma)}\right) < \theta_{ik} \le \dfrac{\pi}{2}, \end{cases}$$

that is, because $f_k$ decreases/increases monotonically in the interval $[0,\gamma]$, we have

$$\begin{aligned}{f_k}^{\max} = \max_{0\le\theta_{ik}\le\gamma} f_k &= \max\{f_k(0), f_k(\gamma)\} \\ &= \max\{-a_{jk}\sin(\gamma), -a_{ik}\sin(\gamma)\} \\ &= -\sin(\gamma)\min\{a_{jk}, a_{ik}\}.\end{aligned}$$

The derivative $\dot{\theta}_{ij}$ can be bounded as

$$\dot{\theta}_{ij} \le \omega_{ij} - 2a_{ij}\sin(\gamma) + \sum_{k\in\mathcal{V}\setminus\mathcal{C}} a_{jk} + a_{ik} + \sum_{k\in\mathcal{C}\setminus\{i,j\}} {f_k}^{\max}.$$

Finally, notice that $\dot{\theta}_{ij} \le 0$ when the angle $\gamma$ satisfies

$$\gamma \ge \arcsin\left(\max_{i,j\in\mathcal{C}}\left(\frac{\omega_{ij} + \sum_{k\in\mathcal{V}\setminus\mathcal{C}} a_{jk} + a_{ik}}{2a_{ij} + \sum_{k\in\mathcal{C}}\min\{a_{jk}, a_{ik}\}}\right)\right),$$

which concludes the proof. □

Theorem 1 implies that the cluster $\mathcal{C}$ is more *cohesive*, that is, it has a smaller angle $\gamma$, when the weight of the edges within the cluster increases. Similarly, the angle $\gamma$ increases when (i) the weight of the edges connecting oscillators within and outside the cluster increases, and (ii) the natural frequencies of the oscillators in the cluster become more heterogeneous ($\omega_{ij}$ increases). It should be noticed that, even in the case $\mathcal{C} = \mathcal{V}$, the angle $\gamma$ may remain positive, that is, the oscillators may not achieve phase synchronization, which is consistent with existing results on networks of heterogeneous oscillators (Dörfler and Bullo (2014)). As can be seen in Fig. 3, the bound $\gamma$ in Theorem 1 may be conservative. A more refined approximation can be obtained by accounting for the natural frequencies of the oscillators outside the cluster, as we show next.

*Lemma 2.* (***Linear comparison***)**.** Let $\mathcal{C}$ be a cluster with respect to the angle $\gamma$. Then at all times,

$$\max_{i,j\in\mathcal{C}}(\theta_j - \theta_i) \le \max_{i,j\in\mathcal{C}}(\tilde{\theta}_j - \tilde{\theta}_i),$$

where $\tilde{\theta}_i$ satisfies $\tilde{\theta}_i(0) = \theta_i(0)$ for all $i \in \mathcal{C}$ and

$$\dot{\tilde{\theta}}_i = \omega_i + \frac{\sin(\gamma)}{\gamma}\sum_{j\in\mathcal{C}} a_{ij}(\tilde{\theta}_j - \tilde{\theta}_i) + \sum_{j\in\mathcal{V}\setminus\mathcal{C}} a_{ij}v_{ij}, \quad (4)$$

with $v_{ij} = \sin(\theta_j - \tilde{\theta}_i)$.

**Proof.** The proof is divided into two parts. First, following the same procedure as in the proof of Theorem 1, it follows that $|\tilde{\theta}_{ij}| = |\tilde{\theta}_j(t) - \tilde{\theta}_i(t)| \le \gamma$ at all times. This part is omitted here in the interest of space. Second, we employ the comparison lemma in Khalil (2002) to prove the claimed statement. Consider the non-negative function

$$g(t,x) := \max(x_j(t) - x_i(t)),$$

where $x_i$ denotes the $i$-th component of the vector $x$. Proving Lemma 2 is equivalent to prove that

$$g(t,\theta) \le g(t,\tilde{\theta}). \quad (5)$$

Let

$$\begin{aligned}\mathcal{U}(t) &= \{i \ : \ \theta_i(t) = \max_j \theta_j(t)\}, \\ \tilde{\mathcal{U}}(t) &= \{i \ : \ \tilde{\theta}_i(t) = \max_j \tilde{\theta}_j(t)\}, \\ \mathcal{L}(t) &= \{i \ : \ \theta_i(t) = \min_j \theta_j(t)\}, \\ \tilde{\mathcal{L}}(t) &= \{i \ : \ \tilde{\theta}_i(t) = \min_j \tilde{\theta}_j(t)\}.\end{aligned}$$

Notice that

$$\begin{aligned}g(t,\theta) &= \theta_i - \theta_j \text{ with } i \in \mathcal{U}(t) \text{ and } j \in \mathcal{L}(t), \\ g(t,\tilde{\theta}) &= \tilde{\theta}_i - \tilde{\theta}_j \text{ with } i \in \tilde{\mathcal{U}}(t) \text{ and } j \in \tilde{\mathcal{L}}(t).\end{aligned}$$

From Lemma 2.2 in Lin et al. (2007), we know that

$$\begin{aligned}D^+ g(t,\theta) &= \limsup_{h\to 0}\frac{g(\theta(t+h)) - g(\theta(h))}{h} \\ &= v_{\max}(t) - v_{\min}(t),\end{aligned}$$

where $D^+ g$ is the right-hand derivative of $g(t,\theta)$, and

$$\begin{aligned}v_{\max}(t) &= \max\{\dot{\theta}_i \ : \ i \in \mathcal{U}(t)\}, \\ v_{\min}(t) &= \min\{\dot{\theta}_i \ : \ i \in \mathcal{L}(t)\}.\end{aligned}$$

Analogously, $D^+ g(t,\tilde{\theta}) = \tilde{v}_{\max}(t) - \tilde{v}_{\min}(t)$. From Lemma 3.3 in Cao and Ren (2011), equation (5) holds if $D^+ g(t,\theta)|_{\theta=\tilde{\theta}} \le D^+ g(t,\tilde{\theta})$. Note that, for some $i^*$ and $j^*$,

$$\begin{aligned}v_{\max} - v_{\min} = \omega_{j^*} - \omega_{i^*} &+ \sum_{k\in\mathcal{C}} a_{j^*k}\sin(\tilde{\theta}_{j^*k}) - a_{i^*k}\sin(\tilde{\theta}_{i^*k}) \\ &+ \sum_{k\in\mathcal{V}\setminus\mathcal{C}} a_{j^*k}\sin(\theta_k - \tilde{\theta}_{j^*}) - a_{i^*k}\sin(\theta_k - \tilde{\theta}_{i^*}),\end{aligned}$$

and,

$$\begin{aligned}\tilde{v}_{\max} - \tilde{v}_{\min} \ge \omega_{j^*} - \omega_{i^*} &+ \frac{\sin(\gamma)}{\gamma}\sum_{k\in\mathcal{C}} a_{j^*k}\tilde{\theta}_{j^*k} - a_{i^*k}\tilde{\theta}_{i^*k} + \\ &+ \sum_{k\in\mathcal{V}\setminus\mathcal{C}} a_{j^*k}\sin(\theta_k - \tilde{\theta}_{j^*}) - a_{i^*k}\sin(\theta_k - \tilde{\theta}_{i^*}).\end{aligned}$$

Thus,

$$\begin{aligned}D^+ g(t,\tilde{\theta}) - D^+ g(t,\theta)|_{\tilde{\theta}} \ge &\sum_{k\in\mathcal{C}} a_{j^*k}\left(\frac{\sin(\gamma)\tilde{\theta}_{j^*k}}{\gamma} - \sin\tilde{\theta}_{j^*k}\right) \\ &- a_{i^*k}\left(\frac{\sin(\gamma)\tilde{\theta}_{i^*k}}{\gamma} - \sin\tilde{\theta}_{i^*k}\right).\end{aligned}$$

Because $|\tilde{\theta}_{ij}| \le \gamma$, we have

$$\begin{cases} \dfrac{\sin(\gamma)\,\tilde{\theta}_{ij}}{\gamma} \le \sin(\tilde{\theta}_{ij}), & \text{if } \tilde{\theta}_{ij} \ge 0, \\ \dfrac{\sin(\gamma)\,\tilde{\theta}_{ij}}{\gamma} \ge \sin(\tilde{\theta}_{ij}), & \text{if } \tilde{\theta}_{ij} \le 0. \end{cases} \quad (6)$$

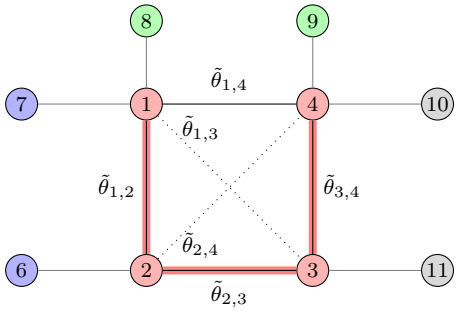


Fig. 2. For the cluster with nodes $\mathcal{C} = \{1, 2, 3, 4\}$ in Fig. 1, this figure shows a spanning tree $\mathcal{T} = (\mathcal{C}, \mathcal{E}_\mathcal{C})$, where $\mathcal{E}_\mathcal{C} = \{(1, 2), (2, 3), (3, 4), (1, 4)\}$. The system (8) associated with the cluster $\mathcal{C}$ is in Example 1.

Notice that, for every $k \in \mathcal{C}$, $\tilde\theta_{i^*} \le \tilde\theta_k \le \tilde\theta_{j^*}$ and, consequently, $\tilde\theta_{i^*k} \ge 0$ and $\tilde\theta_{j^*k} \le 0$. Thus, $D^+g(t, \tilde\theta) - D^+g(t, \theta)\,|_{\tilde\theta} \ge 0$, which concludes the proof. □

### *2.3 Analysis based on approximated linear dynamics*

Lemma 2 shows that the evolution of the nonlinear network dynamics can be bounded by the evolution of the linear system (4) with bounded inputs $v_{ij}$. We use this observation to find a tighter approximation of the clustering angle $\gamma$. Consider a spanning tree $\mathcal{T} = (\mathcal{C}, \mathcal{E}_\mathcal{T})$ of the subgraph $(\mathcal{C}, \mathcal{E}_\mathcal{C})$, with $\mathcal{E}_\mathcal{C} = \mathcal{E} \cap \mathcal{C} \times \mathcal{C}$ (Godsil and Royle (2001)). For $i, j \in \mathcal{C}$, let $p_{ij}$ be the unique path on $\mathcal{T}$ from $i$ to $j$.[1] Let $\tilde\theta_{ij} = \tilde\theta_j - \tilde\theta_i$, and notice that

$$\tilde\theta_{ij} = \sum_{h \in p_{ij}} \tilde\theta_{h+1} - \tilde\theta_h. \tag{7}$$

Let $x_{\text{tree}}$ and $x_{\text{cluster}}$ be the vectors of all $\tilde\theta_{ij}$ with $(i, j) \in \mathcal{E}_\mathcal{T}$ and $(i, j) \in \mathcal{C} \times \mathcal{C}$, respectively, with $j > i$. See Fig. 2 for an illustration of these definitions. Some algebraic manipulation from (4) and (7) leads to

$$\begin{aligned} \dot x_{\text{tree}} &= F x_{\text{tree}} + G u + \Delta_\omega, \\ x_{\text{cluster}} &= H x_{\text{tree}}, \end{aligned} \tag{8}$$

where $F$, $G$, and $H$ are appropriately defined matrices, and $\Delta_\omega$ contains all the differences $\omega_{ij}$ with $j > i$ and $(i, j) \in \mathcal{E}_\mathcal{T}$. Notice that each component $u$ can be written as $u_i = \sin(\theta_p - \tilde\theta_q)$, for some $q \in \mathcal{C}$ and $p \in \mathcal{V} \setminus \mathcal{C}$. The following definition will be used: for the $i$-th component of $u$, let

$$\omega_i^* = |\omega_p - \omega_q|. \tag{9}$$

*Example 1.* ***(An example of system*** (8)***)*** Consider the cluster $\mathcal{C} = \{1, 2, 3, 4\}$ of Fig. 2 with subgraph $(\mathcal{C}, \mathcal{E}_\mathcal{C})$, $\mathcal{E}_\mathcal{C} = \{(1, 2), (2, 3), (3, 4), (1, 4)\}$. The subgraph $\mathcal{T} = (\mathcal{C}, \mathcal{E}_\mathcal{T})$ is a spanning tree, where $\mathcal{E}_\mathcal{T} = \{(1, 2), (2, 3), (3, 4)\}$. The state of the system (8) associated with $\mathcal{T}$ is

$$x_{\text{tree}} = \begin{bmatrix} \tilde\theta_{1,2} & \tilde\theta_{2,3} & \tilde\theta_{3,4} \end{bmatrix}^\mathsf{T},$$
$$x_{\text{cluster}} = \begin{bmatrix} \tilde\theta_{1,2} & \tilde\theta_{2,3} & \tilde\theta_{3,4} & \tilde\theta_{1,4} & \tilde\theta_{1,3} & \tilde\theta_{2,4} \end{bmatrix}^\mathsf{T}.$$

The input $u$ has six components:

$$u_1 = \sin(\theta_7 - \tilde\theta_1), \quad u_2 = \sin(\theta_8 - \tilde\theta_1), \quad u_3 = \sin(\theta_6 - \tilde\theta_2),$$
$$u_4 = \sin(\theta_{11} - \tilde\theta_3), \quad u_5 = \sin(\theta_9 - \tilde\theta_4), \quad u_6 = \sin(\theta_{10} - \tilde\theta_4).$$

[1] A path $p_{ij}$ on $\mathcal{E}_\mathcal{T}$, $i, j \in \mathcal{C}$, is a sequence of vertices of $\mathcal{C}$ such that $i$ and $j$ are the first and last elements of the sequence, respectively, and for any two consecutive nodes $k, h$ it holds $(k, h) \in \mathcal{E}_\mathcal{T}$.

The matrices $F$, $G$, $H$ and the vector $\Delta_\omega$ are as follows:

$$F = \begin{bmatrix} -(2a_{1,2} + a_{1,4}) & (a_{2,3} - a_{1,4}) & -a_{1,4} \\ a_{1,2} & -a_{2,3} & a_{3,4} \\ -a_{1,4} & -(a_{2,3} + a_{1,4}) & -(2a_{3,4} + a_{1,4}) \end{bmatrix},$$

$$G = \begin{bmatrix} -a_{1,7} & -a_{1,8} & a_{2,6} & 0 & 0 & 0 \\ 0 & 0 & -a_{2,6} & a_{3,11} & 0 & 0 \\ 0 & 0 & 0 & -a_{3,11} & a_{4,9} & a_{4,10} \end{bmatrix},$$

$$H = \begin{bmatrix} 1 & 0 & 0 & 1 & 1 & 0 \\ 0 & 1 & 0 & 1 & 1 & 1 \\ 0 & 0 & 1 & 1 & 0 & 1 \end{bmatrix}^\mathsf{T}, \text{ and } \Delta_\omega = \begin{bmatrix} \omega_2 - \omega_1 \\ \omega_3 - \omega_2 \\ \omega_4 - \omega_3 \end{bmatrix}.$$

Finally, $\omega_1^* = |\omega_7 - \omega_1|$, $\omega_2^* = |\omega_8 - \omega_1|$, $\omega_3^* = |\omega_6 - \omega_2|$, $\omega_4^* = |\omega_3 - \omega_{11}|$, $\omega_5^* = |\omega_4 - \omega_9|$, and $\omega_6^* = |\omega_4 - \omega_{10}|$. □

*Lemma 3.* ***(Stability of*** (8)***)*** The system (8) is stable.

**Proof.** Let $\tilde\theta$ be the vector of $\tilde\theta_i$ with $i \in \mathcal{C}$, and let $\dot{\tilde\theta} = -L\tilde\theta + v$, where $L$ and $v$ are defined from (4). Notice that $L$ is a Laplacian matrix (Godsil and Royle (2001)), in fact it equals the Laplacian of the subgraph of $\mathcal{G}$ with nodes $\mathcal{C}$. Thus, because the graph $\mathcal{G}$ is connected, $L$ has a simple eigenvalue at the origin, with eigenvector with all equal components (Olfati-Saber et al. (2007)). Thus, the autonomous dynamics $\dot{\tilde\theta} = -L\tilde\theta$ satisfy

$$\lim_{t\to\infty} \tilde\theta_j(t) - \tilde\theta_i(t) = 0,$$

for all $i, j \in \mathcal{C}$. Thus, the matrix $F$ is stable because, when $\Delta_\omega = 0$ and $u = 0$, the differences $\tilde\theta_{ij}$ converge to zero. □

Next, we exploit the frequency behavior of the system (8) to derive a tighter bound for the cohesiveness of the phases of the oscillators within a cluster.

*Theorem 4.* ***(Approximation based on linearized dynamics)*** Let $G_i$ be the $i$-th column of the matrix $G$ in (8), and $\omega_i^*$ be as in (9). Then, with the same notation as in Lemma 2, $\max_{ij} \theta_{ij} \le \max_{ij} \tilde\theta_{ij} = \|x_{\text{cluster}}\|_\infty$, and [2]

$$\left| \|x_{\text{cluster}}\|_\infty - \left\| HF^{-1}\Delta_\omega + \textstyle\sum_i H(\mathrm{i}\omega_i^* I - F)^{-1} G_i \right\|_\infty \right| \approx 0. \tag{10}$$

**Proof.** To obtain the approximate bound in Theorem 4, we assume that, using the notation in (9),

$$u_i = \sin(\theta_p - \tilde\theta_q) \approx \sin((\omega_p - \omega_q)t) = \sin(\omega_i^* t).$$

We then exploit standard argument from linear system theory, and in particular the harmonic response of a linear system, and stability of (8) to conclude the proof.

It should be observed that our approximation is tighter as the frequencies $\omega_i^*$ grow to infinity while the natural frequencies of the oscillators in the cluster remain bounded. In fact, in this case with appropriate initial conditions we have that $\omega_i$ grows to infinity, with $i \in \mathcal{V}\setminus\mathcal{C}$, and the phase $\theta_i$ evolves as $\omega_i t$:

$$\frac{\dot\theta_i}{\omega_i} = 1 + \underbrace{\sum_{j\in\mathcal{C}} \frac{a_{ij}}{\omega_i} \sin(\tilde\theta_j - \theta_i)}_{\to 0} + \underbrace{\sum_{j\in\mathcal{V}\setminus\mathcal{C}} \frac{a_{ij}}{\omega_i} \sin(\theta_j - \theta_i)}_{\to 0} = 1.$$

Then, we have that $\sin(\theta_p - \tilde\theta_q)$ converges to $\sin(\omega_p t)$, and the symbol $\approx$ in (10) can instead be replaced with $=$. □

[2] In (10) we have $=$ instead of $\approx$ when the cluster comprises all nodes, that is$\mathcal{C} = \mathcal{V}$, when $G = 0$, or $\omega_i^*$ grow to infinity.

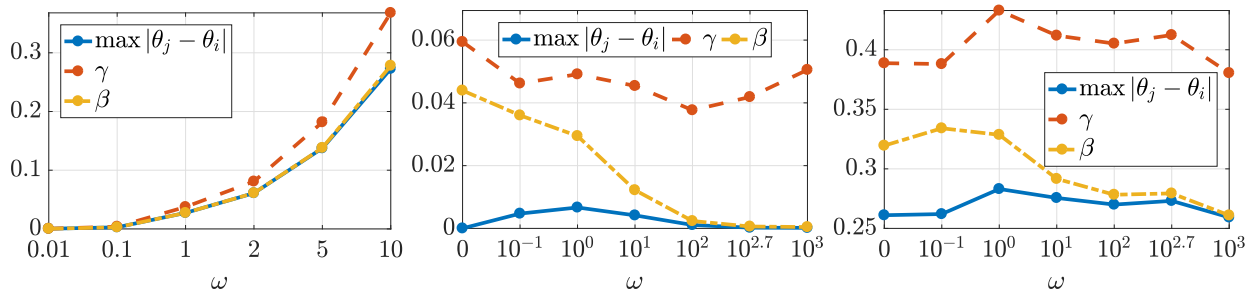


(a) $m = n$ and $\omega_i \leq \omega$, $i \in \mathcal{C}$ (b) $\omega_i = 0$, $i \in \mathcal{C}$ and $\omega_k \leq \omega$, $k \in \mathcal{V} \setminus \mathcal{C}$ (c) $\omega_i \leq 1$, $i \in \mathcal{C}$ and $\omega_k \leq \omega$, $k \in \mathcal{V} \setminus \mathcal{C}$

Fig. 3. This figure shows the largest phase difference among the oscillators in the cluster, as described in Section 3, and the bounds $\gamma$ and $\beta$ derived in Theorem 1 and Theorem 4, respectively. In Fig. (a), the cluster comprises all nodes ($\mathcal{V} = \mathcal{C}$) and, for each value of $\omega$, the oscillators natural frequencies are selected randomly and uniformly distributed in the interval $[0, \omega]$. In Fig. (b), the cluster comprises a proper subset of nodes, the oscillators in the cluster have equal frequency, while the frequencies of the oscillators outside the cluster are selected randomly and uniformly distributed in the interval $[0, \omega]$. In Fig. (c), the cluster comprises a proper subset of nodes, the frequencies of the oscillators in the cluster are selected randomly and uniformly distributed in the interval $[0, 1]$, while the frequencies of the oscillators outside the cluster are selected randomly and uniformly distributed in the interval $[0, \omega]$. Notice that (i) $\beta$ is a tighter bound than $\gamma$, (ii) the cohesiveness of the cluster increases when the frequencies of the oscillators outside the cluster increase, and (iii) exact phase synchronization is possible only when the oscillators in the cluster have equal frequency, and the frequencies of the oscillators outside the cluster increase to infinity.

Theorem 4 shows how the frequency of the oscillators connected to a cluster affects the cohesiveness of the phases of its oscillators. In particular the larger $\omega_i^*$, the less the effect of the of the neighboring oscillators on the cohesiveness of the cluster. In fact, in the limit when all $\omega_i^*$ grow to infinity, the cluster is effectively disconnected from the neighboring agents because the cluster dynamics act as a low pass filter with respect to the frequencies $\omega_i^*$. Additionally, it can be shown that, as all $\omega_i^*$ grow to infinity and $\Delta_\omega$ decreases to zero, the cluster achieves phase synchronization, that is,

$$\lim_{t \to \infty} \max_{i,j \in \mathcal{C}} \theta_j(t) - \theta_i(t) = 0.$$

Finally, it should be noticed that the vector $\Delta_\omega$ is due to heterogeneity of the natural frequencies of the clustered oscillators, and it acts as a constant input to the system (8).

## 3. NUMERICAL EXAMPLES

To validate the results in Section 2, we perform two sets of numerical studies. In Fig. 3 we compare the largest phase difference within a cluster of oscillators with the bounds in Theorems 1 and 4 as a function of the oscillators' natural frequencies. We consider fully connected networks of Kuramoto oscillators, where $\mathcal{V} = \{1, \dots, n\}$ and $\mathcal{C} = \{1, \dots, m\}$; $n$ and $m$ are randonly selected in the intervals $\{2, \dots, 10\}$ and $\{2, \dots, n\}$, respectively. The network weights $a_{ij}$ are independent random variables uniformly distributed in the intervals $[0, 1]$, if $i, j \in \mathcal{C}$, and $[0, 0.01]$ otherwise. For each value of the largest natural frequency $\omega$, we generate 100 different networks, compute the largest phase difference within the cluster, evaluate our bounds, and report the average results. The results show that the bound in Theorem 4 is tighter than the bound in Theorem 1, and that it captures the asymptotic behavior of the phase difference as the natural frequencies of the oscillators outside the cluster increase. Moreover, the cohesiveness of the cluster increases when the frequencies of the oscillators outside the cluster increase, and exact phase synchronization is possible only when the oscillators in the cluster have equal frequency, and the frequencies of the oscillators outside the cluster increase to infinity.

In Fig. 4 we report the time trajectory of the largest phase difference within a cluster. We consider fully connected networks of Kuramoto oscillators, where the network weights $a_{ij}$ are independent random variables uniformly distributed in the intervals $[0, 1]$, if $i, j \in \mathcal{C}$, and $[0, 0.01]$ otherwise. We consider different choices of $\mathcal{V}$, $\mathcal{C}$, and of the oscillators natural frequencies, as described in the figure caption. The results show how the phase differences inside the cluster decrease when the natural frequencies inside the cluster are homogeneous, and when the frequencies of the neighboring oscillators are sufficiently larger.

## 4. CONCLUSION

This paper characterizes cluster synchronization in networks of Kuramoto oscillators as a function of the network weights and oscillators parameters. The paper shows how cluster synchronization depends on a graded combination of strong intra-cluster and weak inter-cluster connections, similarity of the natural frequencies of the oscillators within each cluster, and heterogeneity of the natural frequencies of coupled oscillators belonging to different groups. The technical approach leverages tools from linear and nonlinear control theory, and is numerically validated.

## REFERENCES

Banaie, M., Sarbaz, Y., Pooyan, M., Gharibzadeh, S., and Towhidkhah, F. (2009). Modeling huntingtons disease considering the theory of central pattern generators. In *Advances in Computational Intelligence*, 11–19. Springer.

Burger, M., Zelazo, D., and Allgower, F. (2013). Hierarchical clustering of dynamical networks using a saddle-point analysis. *IEEE Transactions on Automatic Control*, 58(1), 113–124. doi:10.1109/TAC.2012.2206695.

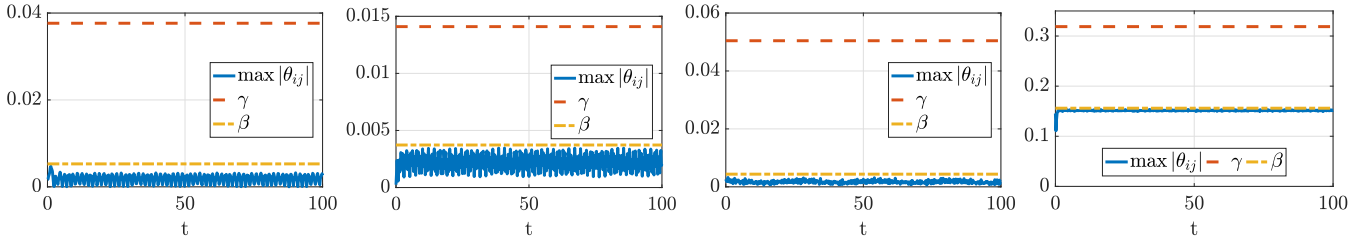


(a) $n=4, m=2, \omega_i = 0, \omega_k \leq 10$ (b) $n=4, m=2, \omega_i \leq 1, \omega_k \leq 10$ (c) $n=20, m=10, \omega_i=0, \omega_k \leq 100$ (d) $n=20, m=10, \omega_i \leq 1, \omega_k \leq 100$

Fig. 4. This figure shows the largest phase difference among the oscillators in the cluster over time (blue, continuous), as described in Section 3. We consider fully connected Kuramoto networks, where $\mathcal{V} = \{1, \ldots, n\}$, $\mathcal{C} = \{1, \ldots, m\}$, $\{\omega_1, \ldots, \omega_m\}$ are selected randomly in the interval $[0, \omega_{\text{in}}^{\max}]$, and $\{\omega_{m+1}, \ldots, \omega_n\}$ are selected randomly in $[0, \omega_{\text{out}}^{\max}]$, with $n = 4$ in Fig. (a) and (b), $n = 20$ in Fig. (c) and (d), $m = 2$ in Fig. (a) and (b), $m = 10$ in Fig. (c) and (d), $\omega_{\text{in}}^{\max} = 0$ in Fig. (a) and (c), $\omega_{\text{in}}^{\max} = 1$ in Fig. (b) and (d), $\omega_{\text{out}}^{\max} = 10$ in Fig. (b), $\omega_{\text{out}}^{\max} = 100$ in Fig. (c) and (d). The figures highlight how heterogeneity of the natural frequencies of the oscillators in the clusters affect cluster cohesiveness. The bound from Theorem 1 is in red (dashed); the bound from Theorem 4 is in yellow (dashed-dot).


Cao, Y. and Ren, W. (2011). Distributed multi-agent coordination: A comparison lemma based approach. In *American Control Conference*, 1618–1623. San Francisco, CA, USA.

Cenedese, A. and Favaretto, C. (2015). On the synchronization of spatially coupled oscillators. In *IEEE Conf. on Decision and Control*, 4836–4841. Osaka, Japan.

Chopra, N. and Spong, M.W. (2005). On synchronization of kuramoto oscillators. In *IEEE Conf. on Decision and Control*, 3916–3922. Seville, Spain.

Dahms, T., Lehnert, J., and Schöll, E. (2012). Cluster and group synchronization in delay-coupled networks. *Physical Review E*, 86, 016202.

Dörfler, F. and Bullo, F. (2014). Synchronization in complex networks of phase oscillators: A survey. *Automatica*, 50(6), 1539–1564.

Ferrari, F.A.S., Viana, R.L., Lopes, S.R., and Stoop, R. (2015). Phase synchronization of coupled bursting neurons and the generalized kuramoto model. *Neural Networks*, 107–118.

Giardina, I. (2008). Collective behavior in animal groups: theoretical models and empirical studies. *HFSP journal*, 2(4), 205–219.

Godsil, C. and Royle, G. (2001). *Algebraic Graph Theory*. Graduate Texts in Mathematics. Springer New York.

Gushchin, A., Mallada, E., and Tang, A. (2015). Synchronization of heterogeneous kuramoto oscillators with arbitrary topology. In *American Control Conference*, 637–644. Chicago, IL, USA.

Hammond, C., Bergman, H., and Brown, P. (2007). Pathological synchronization in parkinson's disease: networks, models and treatments. *Trends in Neurosciences*, 30(7), 357–364.

Khalil, H.K. (2002). *Nonlinear Systems*. Prentice Hall.

Kuramoto, Y. (1975). Self-entrainment of a population of coupled non-linear oscillators. In *International symposium on mathematical problems in theoretical physics*, 420–422. Berlin, Heidelberg.

Kurz, F.T., Derungs, T., Aon, M.A., ORourke, B., and Armoundas, A.A. (2015). Mitochondrial networks in cardiac myocytes reveal dynamic coupling behavior. *Biophysical journal*, 108(8), 1922–1933.

Lehnertz, K., Bialonski, S., Horstmann, M.T., Krug, D., Rothkegel, A., Staniek, M., and Wagner, T. (2009). Synchronization phenomena in human epileptic brain networks. *Journal of Neuroscience Methods*, 183(1), 42–48.

Lewis, F.L., Zhang, H., Hengster-Movric, K., and Das, A. (2014). Introduction to synchronization in nature and physics and cooperative control for multi-agent systems on graphs. In *Cooperative Control of Multi-Agent Systems*, 1–21. Springer.

Lin, Z., Francis, B., and Maggiore, M. (2007). State agreement for continuoustime coupled nonlinear systems. *SIAM Journal on Control and Optimization*, 46(1), 288–307.

Lu, W., Liu, B., and Chen, T. (2010). Cluster synchronization in networks of coupled nonidentical dynamical systems. *Chaos: An Interdisciplinary Journal of Nonlinear Science*, 20(1), 013120.

Nishikawa, T. and Motter, A.E. (2015). Comparative analysis of existing models for power-grid synchronization. *New Journal of Physics*, 17(1), 015012.

Nordenfelt, A., Used, J., and Sanjuán, M.A.F. (2013). Bursting frequency versus phase synchronization in time-delayed neuron networks. *Physical Review E*, 87, 052903.

Olfati-Saber, R., Fax, J.A., and Murray, R.M. (2007). Consensus and cooperation in networked multi-agent systems. *Proceedings of the IEEE*, 95(1), 215–233.

Pecora, L.M., Sorrentino, F., Hagerstrom, A.M., Murphy, T.E., and Roy, R. (2014). Cluster synchronization and isolated desynchronization in complex networks with symmetries. *Nature communications*, 5.

Rubchinsky, L.L., Park, C., and Worth, R.M. (2012). Intermittent neural synchronization in parkinson's disease. *Nonlinear Dynamics*, 68(3), 329–346.

Schaub, M.T., O'Clery, N., Billeh, Y.N., Delvenne, J.C., Lambiotte, R., and Barahona, M. (2016). Graph partitions and cluster synchronization in networks of oscillators. *Chaos*, 26(9), 094821.

Sorrentino, F., Pecora, L.M., Hagerstrom, A.M., Murphy, T.E., and Roy, R. (2016). Complete characterization of the stability of cluster synchronization in complex dynamical networks. *Science Advances*, 2(4).

Strogatz, S.H. (2000). From Kuramoto to Crawford: exploring the onset of synchronization in populations of coupled oscillators. *Physica D: Nonlinear Phenomena*, 143(14), 1–20.